Untangling the Excited States of DR1 in Solution: An Experimental and Theoretical Study

Leonardo De Boni, Carlos Toro, Artëm E. Masunov,‡ and Florencio E. Hernández*,†

Department of Chemistry, University of Central Florida, P.O. Box 162366, Orlando, Florida 382616-2366

Received: December 7, 2007; In Final Form: January 25, 2008

We report the experimental observations and the theoretical predictions of the fully separated n−π* and π−π* bands of Disperse Red One in acidified methanol solution. The analysis of the linear and two-photon absorption spectra is presented in four specific solvents. We demonstrate the possibility to establish the position of the first two excited states combining linear and nonlinear spectroscopy. Calculations using density functional theory at TD-B3LYP/6-31G*//HF/6-31G* level accurately predict the spectral region of the n−π* and π−π* transitions of DR1 in all solvents.

Introduction

Disperse Red One (DR1), shown in Scheme 1, has been extensively studied[1] during the past decade for its photoisomerization properties that have led to multiple applications in optical data storage and optical switching devices.[2,3] According to the shape of the absorption spectra, the azo chromophores have been classified as azobenzene, aminoazobenzene, and pseudo-stilbene types.[4] The optical properties of stilbene are determined by a unique excited-state of π→π* nature, which is symmetry allowed and responsible for their strong absorption and fluorescence.[4] Conversely, the azo (diazene) group (−N═N−) in azobenzene, which is isosteric with the ethene group, presents the additional electron lone pair of the nitrogen atoms. Consequently, the antisymmetric combination of orbitals becomes the highest occupied molecular orbital (HOMO) in azobenzene, giving rise to the dark n→π* state (symmetry forbidden in the case of idealized planar geometry of the molecule). This dark state appears as a totally separated, low-intensity band on the longer wavelength region of the absorption spectrum of azobenzene, well beyond the π→π*. On the other hand, electron-donating substituents red-shift the π→π* band; thus the dark n→π* band overlaps with the former, and it appears as a small shoulder in the aminoazobenzene absorption spectrum. In the case of disubstitution with electron-donating and electron-withdrawing groups in positions 4 and 4′, respectively (push/pull substitution pattern), an even further red-shift of the π→π* band completely covers the dark n→π* band in pseudo-stilbenes azoaromatic dyes.[5] A special case of pseudo-stilbene azocompounds is observed when the diazo group is protonated or metal-coordinated. This protonation strongly blue-shifts the n→π* state, and the π→π* state becomes the lowest-excited singlet state.[6,7] While strong fluorescence was reported for protonated pseudo-stilbenes dyes, very weak emission from push−pull pseudo-stilbenes azocompounds, aminoazobenzene, and azobenzenes has been observed only when low temperature, solid matrix, or the employment of a powerful excitation source has been used.[1]

Even though the dark n→π* state is hidden in push−pull-substituted pseudo-stilbene azoaromatic compounds (such as DR1), the bright π→π* state was traditionally considered to be its lowest-excited singlet state.[1] However, this viewpoint began to change by the mounting evidence, both experimental and theoretical. According to recent transient absorption studies,[8] the bright π→π* state in DR1 is still higher in energy than the longer-lived n→π* state. Theoretical calculations of DR1 in vacuum and different organic solvents, reported by Roitberg's[9] and Brouwer's[8] groups, have also showed that in push−pull azoaromatic compounds the π→π* state is still higher in energy than the dark n→π* one. To resolve this controversy, we studied DR1 in different solvents including a series of alcohols. We demonstrated, experimentally and theoretically, that the π→π* state can be either higher or lower in energy than the n→π* depending upon the host solvent.[10] While polar solvents stabilize the bright π→π* state of DR1, it remains higher in energy than the n→π*, similar to azobenzene.[4] In alcohols, the two transitions are rearranged due to hydrogen bonds formation; thus the bright state (π→π*) becomes indeed the lowest-excited singlet state. This feature was evidenced by fluorescence spectroscopy of DR1 at room temperature.[10] These significant findings have enhanced the understanding of these photoswitching molecules and could change the definition of pseudo-stilbene azoaromatic compounds based on the spectral position of their bright and dark states.[4] In addition, a complete interpretation of our experimental results specified the position of the first two singlet-excited states and showed that the n−π* band remains hidden under the π−π*.[10]

At present, more spectroscopic evidence revealing the spectral region for the transitions of DR1 is needed for a thoughtful characterization of push−pull azoaromatic derivatives. Furthermore, the absolute separation and the identification of the two bands in linear spectra of DR1 is still a challenge for scientists. One could expect multiphoton spectroscopy to reveal the nature of the excited states with greater certainty. Two-photon absorption (2PA) spectroscopy offers new venues for the elucidation of the excited states that are not accessible via one-photon (linear) absorption (1PA).[11] 2PA is based on the simultaneous

SCHEME 1

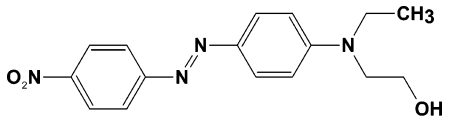

* Corresponding author. E-mail: florenzi@mail.ucf.edu.
† Also with CREOL, the College of Optics and Photonics, UCF.
‡ NanoSciences Technology Center, Department of Chemistry, and Department of Physics, UCF.

10.1021/jp711552e CCC: $40.75 © 2008 American Chemical Society
Published on Web 03/20/2008

absorption of two photons in a single event.[12] A key feature of 2PA is the even-parity selection rule for symmetric molecules, instead of the odd-parity for 1PA. However, most of the 2PA characterization on azoaromatic derivatives has been directed toward the study of their structure−property relationship,[13−15] and their applications to high-density optical data storage systems,[16,17] rather than toward the elucidation of the nature of excited states.

In this Article, we report the experimental and theoretical 1PA and 2PA spectra of DR1 in toluene, phenol, methanol, and acidified methanol. We show for the first time the n−π* band of this azoaromatic compound in acidified methanol. We also demonstrate that 1PA and 2PA in DR1 obey analogous selection rules in most solvents, allowing only excitation to the bright states. Calculations using density functional theory at TD-B3LYP/6-31G*//HF/6-31G* level predict the spectral region of the n−π* and π−π* transitions of DR1 in all solvents.

Materials and Methods

Disperse Red One (Standard Fluka ~95%) (*N*-ethyl-*N*-(2-hydroxyethyl)-4-(4-nitrophenylazo)aniline) from Sigma-Aldrich was used without any further purification. Analytical grade toluene (ACS reagent > 99.8%), liquified phenol (USP testing specifications, ≥89.0% and ~10% H_2O), methanol (ACS reagent >99.8%), and HCl (12 M) were purchased from Sigma-Aldrich and used as they were. These four solvents were specifically selected because the spectral position of the n−π* and π−π* transition of DR1 varies in each of them, as shown later.

The absorbance spectra were taken with a single-beam spectrophotometer (Agilent 8453 Diode Array UV−vis) in a 1 cm quartz cell. The absorbance spectrum of DR1/acidified methanol at a concentration 1000 times greater than in pure solvents was taken in a 100 μm quartz cell. The contribution from the solvent and the quartz cells was subtracted. The degenerated 2PA spectra of DR1 in toluene, phenol, methanol, and acidified methanol (3 mL of HCl (12 M) + 2 mL of DR1/methanol, pH = −0.86) solution were carried out using the well-known open aperture Z-scan technique[18] at different wavelengths. The nonlinear excitation was performed using a tunable OPG pumped by the third harmonic of a mode-locked, 25 ps full-width at half-maximum (fwhm), Nd:YAG laser (EKSPLA), operating at a 10 Hz repetition rate. Typical concentrations of 2.5×10^{-5} and 2.5×10^{-3} M were used for 1PA and 2PA spectra, respectively.

Theoretical Calculation Methods. The 1PA and 2PA profiles were simulated using the approach described in ref 19. The ground-state geometries were optimized at the Hartree−Fock (HF) level with 6-31G* basis set. The electronic structure was calculated at a density functional theory level with the hybrid B3LYP exchange-correlation functional, 6-31G* basis set, and polarizable continuum model (PCM). This combined B3LYP/6-31G*/PCM//HF/6-31G* approach was found[19,20] to provide rotation barriers, geometries, and excitation energies, which agree well with experiment for stilbene and its derivatives. TD-DFT formalism[21] implemented in the Gaussian 98 program package[22] was used to calculate the excitation energies (Ω), corresponding transition densities (ξ), and two-electron (Coulomb) integrals (V) on these densities. The calculated values were input into a modified collective electronic oscillator (CEO) program[23] to calculate first- and third-order polarizabilities $\alpha(\omega; \omega)$ and $\gamma(-\omega; \omega, \omega, -\omega)$, respectively. At frequency ω, the 1PA absorptivity is given by the imaginary part of the linear polarizability

$$\alpha(\omega) = \sum_{\nu} \frac{2\Omega_{\nu}\mu_{g\nu}\mu_{g\nu}^{*}}{\Omega_{\nu}^{2} - (\omega + i\Gamma)^{2}} \tag{1}$$

where $\mu_{g\nu}$ is the transition dipole moment, corresponding to the $|g\rangle$ to $|\nu\rangle$ electronic transition, Ω_{ν} is the vertical transition frequency, and Γ is the empirical line width parameter, assumed to be 0.1 eV for all of the calculations. The 2PA cross section (σ_2) is a function of the imaginary part of the third-order polarizability $\gamma(-\omega; \omega, \omega, -\omega)$,[23]

$$\sigma^{2}(\omega) = \frac{4\pi^{2}\hbar\omega^{2}}{n^{2}c^{2}} L^{4} \mathrm{Im}\langle\gamma(-\omega,\omega,\omega,-\omega)\rangle \tag{2}$$

where $\hbar$ is Planck's constant, n is the refractive index of the medium, c is the speed of light, and L is the local field factor. The term

$$\langle\gamma\rangle = \frac{1}{15}\left(3\sum_{i}\gamma_{iijj} + \sum_{i\neq j}(\gamma_{iijj} + \gamma_{iiji} + \gamma_{ijij})\right) \tag{3}$$

is the orientationally averaged third-order polarizability γ, in which i and j refer to the spatial directions x, y, and z. Eight-term expression for the third-order polarizability, in the CEO formalism, was derived for the TD-HF[21] and TD-DFT[24] theory levels. Unlike the sum over state TD−DFT approach,[25,26] CEO does not require quadratic response properties, such as transition dipole moments between excited states.

The first 24 singlet excited states were taken into account in all calculations. In the previous study of similar conjugated molecules, 11 states were found to be sufficient to reach asymptotic values in resonant third-order response properties.[27]

To account for solvent polarity, self-consistent reaction field approach was used.[10] Nonequilibrium solvation model and integral equation formalism within polarizable continuum model (IEF-PCM) were employed. In this approach, the molecular-shaped cavity is built around the solute. In the solute molecule, the charge distribution induces dielectric response from polarizable continuum outside of the cavity. This response results in the set of effective charges distributed over the cavity surface. These charges are then included in the molecular Hamiltonian and affect the energies and electronic structures of the ground and excited states. The accurate calculations of solvatochromic shifts in protic solvent by polarizable continuum models require the specific solvent effects taken into account using H-bonded aggregated clusters rather than bare solute molecules surrounded by the dielectric continuum.[28,29] To this extent, three solvent molecules (either phenol or methanol) were explicitly added to the DR1 molecule to form a cluster (one H-bond for each nitrogen atom), which was treated at the theory level described above. The addition of extra solvent molecules H-bonded to the nitrogen atoms or the nitro groups did not have an appreciable effect on the excitation wavelength or transition dipoles. The protonated species were designed by adding one proton to the N atom of the amino- or diazo-group and reversing the corresponding H-bonded alcohol molecule from H-donating to H-accepting orientation. This protonation resulted in dissociation of the two remaining H-donating molecules during the optimization, and the results for the protonated species are reported with one explicit solvent molecule.

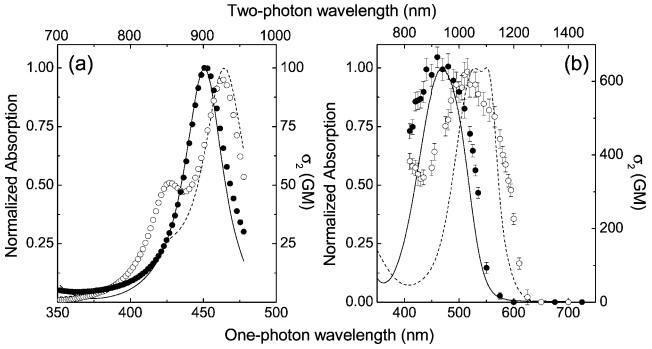

Figure 1. (a) Theoretical spectra of DR1 in solution: 1PA (−) and 2PA (●) in toluene; 1PA (- - -) and 2PA (○) in phenol. (b) Experimental spectra of DR1 in solution: 1PA (−) and 2PA (●) in toluene; 1PA (- - -) and 2PA (○) in phenol.

Results and Discussion

In Figure 1, we show the 1PA and 2PA spectra of DR1 in toluene and phenol. The theoretical linear and nonlinear absorption spectra (Figure 1a) of DR1 in toluene show a close overlap, while in phenol the overlap only holds above approximately 440 nm, and another 2PA state of $\pi-\pi^*$ nature, not active in 1PA, appears at 420 nm. Detailed analysis of excited-state configurations shows that each of 2PA active states presents a mixture of HOMO−LUMO transition and charge-transfer excitation from one of the phenol molecules to LUMO of DR1. According to our calculations, the nature of the lowest bright ($\pi-\pi^*$) and dark (n$-\pi^*$) transitions does not depend on the solvent. In Table 1, we report the theoretical values of the oscillator strength (f) and 2PA cross sections (σ_2) of DR1 in toluene and phenol for these states, as well as higher-lying bright states. These results indicate that unless one can thoroughly separate $\pi-\pi^*$ and n$-\pi^*$ bands, the only transition apparently visible in either 1PA or 2PA spectra is the $\pi-\pi^*$ one.

To corroborate the forecasted results, we measured the 1PA and 2PA spectra of DR1 in toluene and phenol solutions. Figure 1b shows the expected overlap between the linear and nonlinear absorption spectra of DR1 in each solvent. Also, one can notice that the 2PA spectrum of DR1/phenol is slightly blue-shifted with respect to its linear absorption counterpart and that a second peak at shorter wavelength (<434 nm) emerges. The latter corresponds to a higher $\pi-\pi^*$(n) transition, predicted theoretically (Figure 1a) and recently observed by Hernández and co-workers.[10] Agreement between theory and experiment allows us to assign the higher 2PA state as intermolecular charge transfer and exclude vibronic coupling between the ground and the first excited state, which can be suggested[30] as a source of an additional band. A remarkable feature is the fact that while the experimental 1PA curve of DR1/toluene is broader, its maximum appears at the predicted wavelength. Nonetheless, DR1/phenol presents its 1PA maximum at a longer wavelength than the theoretical spectrum. In experimental curves, the inhomogeneous spectral broadening is always anticipated at room temperature and in solution. The spectral red shift of DR1 in phenol can be attributed to partial protonation of DR1 in a weak acid solution.[10,31] The differences between the theoretical and the experimental σ_2 values (see Table 1) are attributed to the pulse width (ps) provided by the laser system. As it was shown by Belfield and co-workers,[32] the 2PA cross section obtained with picosecond pulses is approximately 5−10-fold larger than that found with femtosecond pulses due to substantial excited-state absorption. At shorter wavelengths, 2PA measurements were not performed because resonance enhancement effects become exceedingly high.

In Figure 2, we present the theoretical and experimental 1PA and 2PA spectra of DR1 in methanol and acidified methanol. Calculations in the former (Figure 2a), considering the formation of hydrogen bonds between methanol and the azo-nitrogens of DR1, show that the $\pi-\pi^*$ transition (S_1) is centered at 506 nm. The n$-\pi^*$ (S_2) transition, centered at 442 nm, is not revealed in Figure 2a because it is a dark transition (Table 1) and it remains hidden under S_1 band.[8] In the UV region, other small bands appear at 294 and 343 nm, corresponding to higher energy $\pi-\pi^*$(n) transitions. In DR1/acidified methanol, the theoretical calculations were performed considering two different scenarios: (a) protonation of one of two azo-nitrogens, and (b) protonation of the amino group in position 8. In the former, neither the order of the excited states nor the oscillator strengths alters significantly (data not showed). In the latter, protonation of the amino group eliminates the $\pi-\pi^*$ state completely (Figure 2b), and breaks H-bonds between the methanol molecules and diazo group, making the molecule more flexible.

TABLE 1: Theoretical Oscillator Strength (f) and 2PA Cross-Section (σ_2) Values at the Corresponding Transition Wavelengths (λ), and Experimental Peak Absorption Wavelengths (λ_{Exp}) and σ_2 for Each Transition

DR1		theoretical			experimental	
solvent	transition	λ (nm)	f	σ_2 (GM)	λ_{Max} (nm)	σ_2 (GM)
toluene	$\pi-\pi^*$(n)	325	0.25	153	278[a]	
		281	0.23	209		
	$\pi-\pi^*$	454	0.93	82	434	650
	n$-\pi^*$	508	0.00			
phenol	$\pi-\pi^*$(n)	427	0.09	57	330	
	$\pi-\pi^*$	461	0.75	101	526−548	600
	n$-\pi^*$	452	0.00			
methanol	$\pi-\pi^*$(n)	347	0.30	92	275	
		285				
	$\pi-\pi^*$	473	0.82	105	487	620
	n$-\pi^*$	442	0.02			
acidified methanol	$\pi-\pi^*$(n)	331	1.05		270−334	
		360	0.06	334		
	$\pi-\pi^*$				514−532	280
	n$-\pi^*$	708	0.03		677	0

[a] Reference 10.

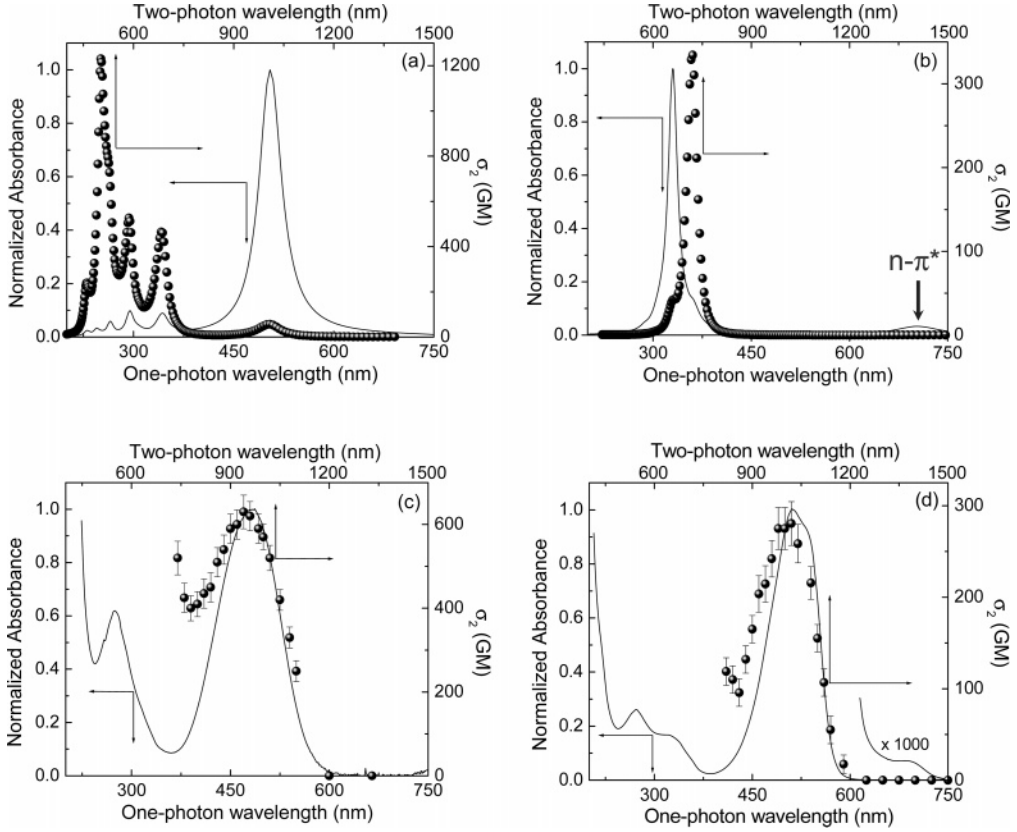

Figure 2. Theoretical 1PA (−) and 2PA (●) spectra of DR1 in methanol (a) and acidified methanol (b). Experimental 1PA (−) and 2PA (●) spectra of DR1 in methanol (c) and acidified methanol (d).

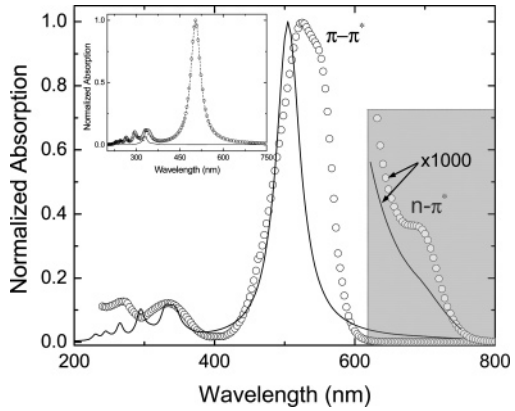

Figure 3. Theoretical absorbance spectra of a mixture of 92% DR1 in methanol (- - -) and 8% DR1 in acidified methanol (−). The "○" correspond to the total absorbance spectrum of the mixture. The inset shows the experimental (−) absorption spectrum of DR1 in acidified methanol and the total theoretical spectrum of the mixture (○). Gray square is ×1000 zoom out.

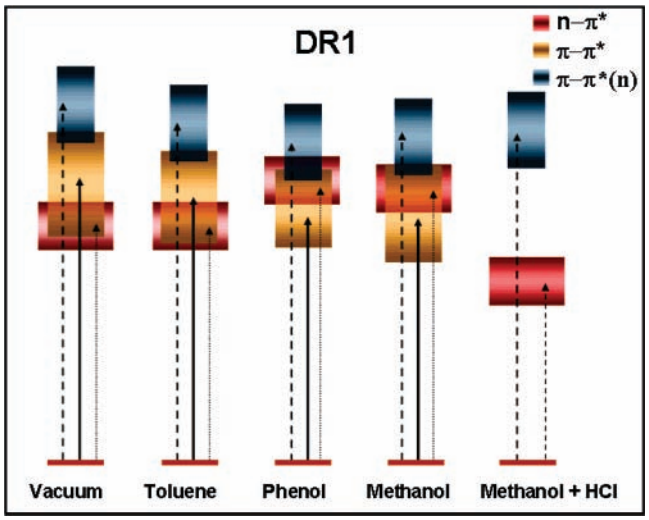

Figure 4. Energy schematic displaying the first three excited states of DR1 in vacuum, toluene, phenol, methanol, and acidified methanol. n−π* (red), π−π* (yellow), and π−π*(n) (blue).

Therefore, this amino-protonation scenario was adopted for the interpretation of our experimental results. The greater basicity of the amino group and its steric accessibility for protonation than those of the diazene group supports our hypothesis of preferential protonation of the amino group.[33] Assuming protonation of the amino group throughout the calculations, we found these results to be in agreement with the trend observed experimentally, although the spectral position of the n−π* band did not match the experimental value exactly. Therefore, calculations at slightly distorted conformations were performed to match the experimental spectra. Slight (15°) shift along inversion coordinate (C−N═N angle) then can stabilize the dark state down to 700 nm, and a 10° twist along CNNC dihedral angle enhances the oscillator strength of the dark transition to 0.04. This deformation corresponds to ca. 2.5 kcal/mol increase of the total energy, which is thermally accessible at room temperature. The greater flexibility can be interpreted as a decrease of the bond order along the central N═N bond in protonated DR1 due to charge delocalization from the azo-nitrogens to the periphery. This effect confers degree of freedom to the molecule at the center.

Figure 2a evidences the extraordinary spectral overlap between the theoretical 1PA and 2PA spectra of DR1/methanol. On the other hand, in Figure 2b, the protonated DR1 in acidified methanol presents totally different 1PA and 2PA spectra. This

theoretical result suggests that by combining linear and 2PA spectroscopy one could elucidate the position of the excited states of DR1 in acidified methanol.

To confirm the latter statement, we show the experimental 1PA and 2PA spectra of DR1 in methanol (Figure 2c) and in acidified methanol (Figure 2d). DR1/methanol presents one band in the UV at 275 nm and one in the visible at 483 nm. A good agreement between the theoretical and experimental spectra of DR1/methanol as well as a close overlap between the experimental 1PA and 2PA spectra were obtained. In contrast, DR1/acidified methanol presents two absorption bands in the UV at 270 and 334 nm, one in the visible at 525 nm, and one close to the near-IR (NIR) at approximately 677 nm. It can be noticed that in DR1/acidified methanol, the experimental and theoretical spectra differ significantly. This can be understood based on the fact that DR1 in acidified methanol exists as a mixture of the protonated and unprotonated forms. Although in acidified methanol solution, the proton concentration is high at pH = −0.86, a much larger concentration of methanol molecules competes for these protons with the small amount of solute molecules (the tertiary amine attached to DR1). Relatively weak basicity of the tertiary amines[33] also contributes to this competition.

To corroborate our hypothesis of partial protonation, we plotted the individual and sum of the theoretical spectra of DR1 considering a mixture of 92% unprotonated and 8% protonated DR1 in solution (Figure 3). The percentages of the species present in solution have been established through the amplitude of the theoretical bands (Figure 2a and b) that fits better the experimental curve of DR1 in acidified methanol (inset Figure 3). The good agreement between the theoretical and experimental spectra indicates the presence of both species in the acidified solution. The assignment of experimental spectrum can be made based on comparison with the two theoretical ones. It includes two absorption bands in the UV, one at 294 and one at 332 nm, one in the visible at 506 nm, and one close to the NIR at 677 nm. The band at 332 nm (absent in pure methanol) as well as the n−π* band in the NIR reveal the presence of the protonated DR1 in acidified methanol. In contrast, the observed strong fluorescence emission at ca. 580 nm confirms the presence of unprotonated DR1 in the acidified methanol solution (data not shown).[10]

Figure 4 shows a scheme illustrating the first three excited states of DR1 in vacuum, toluene, phenol, methanol, and acidified methanol. The overlap of the n−π* and π−π* states illustrates that the total separation of these two states is impossible in the first four environments.[9,10] Yet, the protonated DR1 in acidified methanol exhibits a total separation of the n−π* transition from the π−π*(n) band. The position and width of the absorption bands, corresponding to each transition, were estimated on the basis of the theoretical values of the maximum wavelength of 1PA in each solvent and the corresponding Gaussian spectral deconvolution method (GSDM) of the linear absorption experimental bands, respectively.[10]

Conclusions

In summary, the systematic experimental and theoretical study of DR1 in different solutions has revealed the isolated n→π* band in acidified methanol. We have shown that while the 1PA can take place between the ground state and n→π* and π−π*, 2PA can only occur into the bright π−π* states. This is to our knowledge the first time that n−π* has been entirely separated and experimentally observed in DR1. Additionally, the presence of the weak n−π* band in the red region of the visible demonstrates that both transitions are sensitive to protonation.

Acknowledgment. This research was supported by startup funds provided to F.E.H. by the Department of Chemistry, University of Central Florida. L.D.B. would like to acknowledge CAPES for financial support through Project 4169/06-9. A.E.M. is grateful to the National Science Foundation (CCF-0740344) and Nanoscience Technology Center of University of Central Florida for partial support of this research, and to UCF I2Lab and DOE NERSC for generous donation of computer time.

References and Notes

(1) Sekkat, Z.; Knoll, W. *Photoreactive Organic Thin Films*; Academic Press: New York, 2002.
(2) Natansohn, A.; Rochon, P. *Chem. Rev.* **2002**, *102*, 4139−4175.
(3) Liu, Z.; Hashimoto, K.; Fujishima, A. *Nature* **1990**, *347*, 658−660.
(4) Rau, H. Photoisomerization of Azobenzenes. In *Photochemistry & Photophysics*; Rabek, J. F., Ed.; CRC Press: Boca Raton, FL, 1990; pp 119−141.
(5) Ho, M.-S.; Natasohn, A.; Barreg, C.; Rochon, R. *Can. J. Chem.* **1995**, *73*, 1773−1778.
(6) Haselbach, E. *Helv. Chim. Acta* **1970**, *53*, 1526−1543.
(7) Haselbach, E.; Heilbronner, E. *Tetrahedron Lett.* **1967**, *8*, 4531−4535.
(8) Poprawa-Smoluch, M.; Baggermann, J.; Zhang, H.; Maas, H. P. A.; De Cola, L.; Brouwer, M. *J. Phys. Chem. A* **2006**, *110*, 11926−11937.
(9) Crecca, C.; Roitberg, A. *J. Phys. Chem. A* **2006**, *110*, 8188−8203.
(10) Toro, C.; Thibert, A.; De Boni, L.; Masunov, A. M.; Hernandez, F. E. *J. Phys. Chem. B* **2008**, *112*, 929−937.
(11) Antonov, L.; Kamada, K.; Ohta, K.; Kamounah, F. *Phys. Chem. Chem. Phys.* **2003**, *5*, 1193−1197.
(12) Göppert-Meyer, M. *Ann. Phys.* **1931**, *9*, 273−294.
(13) De Boni, L.; Misoguti, L.; Zilio, S.; Mendonca, C. *ChemPhysChem* **2005**, *6*, 1121−1125.
(14) De Boni, L.; Piovesan, E.; Misoguti, L.; Zilio, S. C.; Mendonca, C. R. *J. Phys. Chem. A* **2007**, *111*, 6222−6224.
(15) Cherioux, F.; Audebert, P.; Maillotte, H.; Grossard, L.; Hernandez, F. E.; Lacourt, A. *Chem. Mater.* **1997**, *9*, 2921−2927.
(16) Ishitobi, H.; Sekkat, Z.; Kawata, S. *J. Chem. Phys.* **2006**, *125*, 164718.
(17) Maeda, M.; Ishitobi, H.; Sekkat, Z.; Kawata, S. *Appl. Phys. Lett.* **2004**, *85*, 351−353.
(18) Sheik-Bahae, M.; Said, A.; Wei, T.; Hagan, D.; Van Stryland, E. *IEEE J. Quantum Electron.* **1990**, *26*, 760−769.
(19) Masunov, A. M.; Tretiak, S. *J. Phys. Chem. B* **2004**, *108*, 899−907.
(20) Masunov, A. M.; Tretiak, S.; Hong, J. W.; Liu, B.; Bazan, G. C. *J. Chem. Phys.* **2005**, *122*, 224506.
(21) Stratmann, R. E.; Scuseria, G. E.; Frisch, M. J. *J. Chem. Phys.* **1998**, *109*, 8218−8224.
(22) Frisch, M. J.; et. al. *Gaussian 98*, revision A.11; Gaussian, Inc.: Pittsburgh, PA, 1998.
(23) Tretiak, S.; Mukamel, S. *Chem. Rev.* **2002**, *102*, 3171−3212.
(24) Tretiak, S.; Chernyak, V. *J. Chem. Phys.* **2003**, *119*, 8809−8823.
(25) Cronstrand, P.; Jansik, B.; Jonsson, D.; Luo, Y.; Agren, H. *J. Chem. Phys.* **2004**, *121*, 9239−9246.
(26) Day, P. N.; Nguyen, K. A.; Pachter, R. *J. Chem. Phys.* **2006**, *125*, 094103.
(27) Kobko, N.; Masunov, A. M.; Tretiak, S. *Chem. Phys. Lett.* **2004**, *392*, 444−451.
(28) Improta, R.; Barone, V. *J. Am. Chem. Soc.* **2004**, *126*, 14320−14321.
(29) Liu, T.; Han, W.-G.; Himo, F.; Ullmann, G. M.; Bashford, D.; Toutchkine, A.; Hahn, K.; Noodleman, L. *J. Phys. Chem. A* **2004**, *108*, 3545−3555.
(30) Rumi, M.; Ehrlich, J. E.; Heikal, A. A.; Perry, J.; Barlow, S.; Hu, Z.; McCord-Maughon, D.; Parker, T.; Rockel, H.; Thayumanavan, S.; Marder, S.; Beljonne, D.; Bredas, J.-L. *J. Am. Chem. Soc.* **2000**, *122*, 9500−9510.
(31) Marino, I.; Bersani, D.; Lottici, P.; Tosini, L.; Montenero, A. *J. Raman Spectrosc.* **2000**, *31*, 555−558.
(32) Belfield, K.; Bondar, M.; Hernandez, F. E.; Przhonska, O.; Yao, S. *J. Phys. Chem. B* **2007**, *111*, 12723−12729.
(33) Solomon, T.; Fryhle, C. *Organic Chemistry*; Wiley: New Jersey, 2007.